



A mathematical model that combines chemotherapy and oncolytic virotherapy as an alternative treatment against a glioma

E. Urenda-Cázares¹ · A. Gallegos¹ · J. E. Macías-Díaz²

Received: 19 July 2019 / Accepted: 16 November 2019 / Published online: 22 November 2019
© Springer Nature Switzerland AG 2019

Abstract

In this paper, we propose a mathematical model that combines chemotherapy and oncolytic virotherapy as an alternative to treatment of a glioma. The main idea is to incorporate the virotherapy after the first or second chemotherapy session using a *specialist* virus that attacks only tumor cells. Some simulations are presented. Based on the results, we conclude that with this combined therapy may reduce the number of chemotherapy sessions and may lead to obtain better results in the fight against gliomas.

Keywords Cancer therapy · Glioma · Nonlinear system of ordinary differential equations · Virotherapy and chemotherapy

1 Introduction

The gliomas are the most common brain tumors and are originated in glial cells [1]. Some gliomas are very aggressive, carrying a rate mortality rate nearing the 100% of the cases within 6–12 months after being diagnosed [2,3]. Usually, the first treatment against gliomas consists of a surgery followed by chemotherapy and radiotherapy, but

✉ E. Urenda-Cázares
ernesto.urenda@academicos.udg.mx

A. Gallegos
gallegos@culagos.udg.mx

J. E. Macías-Díaz
jemacias@correo.uaa.mx

¹ Departamento de Ciencias Exactas y Tecnología, Centro Universitario de los Lagos, Universidad de Guadalajara, Enrique Díaz de León 1144, Colonia Paseos de la Montaña, Lagos de Moreno, Jalisco, Mexico

² Departamento de Matemáticas y Física, Universidad Autónoma de Aguascalientes, Avenida Universidad 940, Ciudad Universitaria, 20131 Aguascalientes, Ags., Mexico

results are far from being effective [4]. Regarding the chemotherapy, the most common agent against brain tumors is the temozolamide [5,6]. There are other proposed treatments based on virotherapy [7], and it has been suggested that the combination of different types of therapies could be a successful alternative, in particular, the combination of chemotherapy and virotherapy [8–10].

On the other hand, the mathematical modeling of cancer has been an essential tool to understand this problem. Moreover, the mathematical approach also allows to replace laboratory experiments and to simulate them computationally. In this sense, scientists have developed a wide diversity of mathematical models covering various aspects of tumor growth (see [11–13] and references therein). In particular case of gliomas, one can find several mathematical proposals [14,15] focusing on the diagnostic [4,16], the chemotherapy [17–19] or the virotherapy [20–23].

In the present work, we propose a mathematical model that combines chemotherapy and oncolytic virotherapy as an alternative treatment against gliomas. The paper is organized as follows. In Sect. 2, the mathematical model is proposed in full detail. Moreover, suitable physical constraints and parameter values are provided. In Sect. 3, a stability analysis of the model associated to the virotherapy is performed. Some simulations are presented in Sect. 4, and the main results are discussed. Finally, we close the article with a brief section of conclusions.

2 Mathematical model

As we mentioned before, the mathematical model proposed in this work consists of two alternative treatments, namely, chemotherapy and virotherapy. The chemotherapy is based on the model proposed by Iarosz et al. [17]. More precisely, a system of differential equations is used to model a brain tumor (more specifically, a glioma), and the corresponding interactions among glial cells, glioma, neurons and chemotherapy. However, in order to match this model with the virotherapy treatment, it is more convenient to state the variables in terms of the number of cells instead of concentrations. Therefore, it is necessary to rescale the parameters of the model.

The rescaling mentioned above can be performed taking into account that the carrying capacity of tumor cells is $k_C = 1.47 \times 10^{12}$ cells [22]. A population of 4.2×10^9 cells corresponds approximately to one tumor of 2 cm of diameter. Assuming a mass per cell of 10^{-12} kg, the corresponding carrying capacity in terms of the concentration is equal to $K_C = 125.3 \text{ kg/m}^3$. In other words, an adequate scale factor is equal to $\delta = 1.17 \times 10^{10} \text{ m}^3 \text{ cells/kg}$. As a consequence, we rescale the set of equations 1-4 in [17] as follows

$$\frac{dG(t)}{dt} = \Omega_1 G(t) \left(1 - \frac{G(t)}{k}\right) - \psi_1 G(t)C(t) - \frac{p_1 G(t)Q(t)}{a_1 + G(t)}, \quad (1)$$

$$\frac{dC(t)}{dt} = \Omega_2 C(t) \left(1 - \frac{C(t)}{k}\right) - \psi_2 G(t)C(t) - \frac{p_2 C(t)Q(t)}{a_2 + C(t)}, \quad (2)$$

$$\frac{dN(t)}{dt} = \bar{\psi} \dot{G}(t)H(-\dot{G})N(t) - \frac{p_3 N(t)Q(t)}{a_3 + N(t)}, \quad (3)$$

Table 1 Parameter values used in the equations (1)–(4)

Description	Parameter	Values	Comment, reference
Proliferation rate	Ω_1	0.0068 day^{-1}	$\Omega_1 < \Omega_2$ [24]
	Ω_2	0.012 day^{-1}	[25]
Loss influences	$\bar{\psi}$	$3.418 \times 10^{-13} \text{ (cells)}^{-1}$	Estimated [17,22]
Interaction coefficients	p_1	$2.808 \times 10^5 \text{ m}^2 \text{ (mg day)}^{-1} \text{ cells}$	[17,22]
	p_2	$2.808 \times 10^8 \text{ m}^2 \text{ (mg day)}^{-1} \text{ cells}$	$p_2 > p_1$ [17,22]
	p_3	$2.808 \times 10^5 \text{ m}^2 \text{ (mg day)}^{-1} \text{ cells}$	$p_3 = p_1$
Chemotherapy agent rate	ζ	0.2 day^{-1}	[26,27]
Holling type 2	a_1, a_2, a_3	$6 \times 10^{12} \text{ cells}$	$a_1 = a_2 = a_3 = k$ [17,22]
Competition coefficients	ψ_1	$3.0769 \times 10^{-15} \text{ (cells day)}^{-1}$	[17,22]
	ψ_2	$3.0769 \times 10^{-16} \text{ (cells day)}^{-1}$	$\psi_2 < \psi_1$
Carrying capacity	k	$6 \times 10^{12} \text{ cells}$	[17,22]

$$\frac{dQ(t)}{dt} = \Phi - \zeta Q(t), \quad (4)$$

where the new parameters are defined in terms of those used in [17] as

$$\bar{\psi} = \frac{\psi}{\delta}, \quad \psi_i = \frac{\Psi_i}{\delta}, \quad p_i = \delta P_i, \quad a_i = \delta A_i, \quad k = \delta K. \quad (5)$$

Table 1 shows the corresponding values of the new parameters.

The variables $G(t)$, $C(t)$ and $N(t)$ correspond to the number of glial cells, glioma cells and neuron cells, respectively, and $Q(t)$ is the concentration of the chemotherapeutic agent given in mg/m^2 . According to [17], the first term in (1) and (2) models a logistic growth of the glial and glioma cells, while the second describes the competition between the two types of cells, and the third models the effect of the chemotherapy on the cells in terms of the Holling type functions [28,29].

The dynamics of number of neuron cells is described by Eq. (3). In that equation, the first term models the decrease of neurons as a consequence of the glial cells death. Here, $H(t)$ is the well-known Heaviside function, which is defined as

$$H(x) = \begin{cases} 0, & x < 0, \\ \frac{1}{2}, & x = 0, \\ 1, & x > 0. \end{cases} \quad (6)$$

Meanwhile, the second term is the effect of the chemotherapy on the neurons.

Finally, Eq. (4) describes the evolution of the concentration of the chemotherapeutic agent. The first term is the function Φ , which is defined as a periodic step function. More specifically, Φ has a constant value of $400 \text{ mg}(\text{m}^2 \text{ day})^{-1}$ during 5 days (chemotherapy session), and is switched off for 23 days, and so on (temozolomide is one of the most common chemotherapeutic agents against brain tumors [5,6]).

In turn, the second term of equation (4) models the corresponding decrease of the agent.

The second part of the model corresponds to the oncolytic virotherapy. This therapy is provided on day 21 (16 days after of the ending of the chemotherapy session) in order to reduce the effects of the agent on the virus. Moreover, this is done in view that the effectiveness of the virotherapy lasts around one week. This part of the model is based on the work of [22]. However, we have considered some additional assumptions and modifications. Concretely, the system of equations is provided as follows:

$$\frac{dC_S(t)}{dt} = \Omega_2 C_S(t) \left(1 - \frac{(C_S(t) + C_I(t))}{k} \right) - \psi_2 G(t) C_S(t) - \frac{p_2 C_S(t) Q(t)}{a_2 + C_S(t)} - C_S(t) \beta_C v(t), \quad (7)$$

$$\frac{dC_I(t)}{dt} = \beta_C C_S(t) v(t) - \lambda_C C_I(t), \quad (8)$$

$$\frac{dv(t)}{dt} = b_C \lambda_C C_I(t) - \beta_C C_S v(t) - \omega v(t). \quad (9)$$

The glial cells equation (1), the neurons equation (3) and the agent equation (4) remain unchanged. We assume that the virus is *specialist*, which means that only infects glioma cells. As a consequence, the tumor cells are divided in healthy $C_S(t)$ and infected $C_I(t)$ by the viruses $v(t)$. The last term in (7) corresponds to the competition between healthy tumor cells and the viruses. We assume that the infected tumor cells cannot reproduce, so that it is important to change $C(t)$ for $C_S(t)$ in (1). In (8) the first term corresponds to the infection of healthy cells as a consequence of the competition with the virus, while the last term is the lysing of the infected cells.

The virus equation (9) describes the releasing of the infection by means of the infected cells. The second term is the competition with healthy cells, and the last one is the clearing of the viruses by the immune response. For simplicity we have dropped the chemotherapy agent effect (which it is minimal between day 21 and 28) in Eqs. (8) and (9). Of course at the beginning of the virotherapy we suppose that $C_S(21) = C(21)$ and $C_I(21) = 0$. The new parameters used in the equations are similar to those used in [22], but written in days units as one can see in the Table 2. Note that three different types of oncolytic viruses are taking account [22]. They are based on some previous works in the literature [7,20,30,31].

3 Local stability

Before we provide some computational simulations, we perform a local stability analysis of the model when the virotherapy is supplied.

Let us suppose that $E(\bar{G}, \bar{C}_S, \bar{C}_I, \bar{N}, \bar{Q}, \bar{v})$ is an equilibrium point which is a solution of the following system:

$$\frac{dG}{dt} = \Omega_1 G(t) \left(1 - \frac{G(t)}{k} \right) - \psi_1 G(t) C_S(t) - \frac{p_1 G(t) Q(t)}{a_1 + G(t)} = 0, \quad (10)$$

Table 2 Parameter values used in Eqs. (7)–(9) (see [22])

Virus	Description	Parameter	Value
Adenovirus (ONYX-15)	Lysing rate of tumor cells	λ_C	$0.5 \text{ cell}^{-1} \text{ day}^{-1}$
	Burst size from lysing infected tumor	b_C	1000
	Viral clearance rate	ω	$24 \text{ virus}^{-1} \text{ day}^{-1}$
	Uptake/encounter/infection rate of tumor cells	β_C	$1.2 \times 10^{-10} \text{ viruses cell}^{-1} \text{ day}^{-1}$
HSV	Lysing grate of tumor cells	λ_C	$4/3 \text{ cell}^{-1} \text{ day}^{-1}$
	Burst size from lysing infected tumor	b_C	50
	Viral clearance rate	ω	$0.6 \text{ virus}^{-1} \text{ day}^{-1}$
	Uptake/encounter/infection rate of tumor cells	β_C	$6 \times 10^{-11} \text{ viruses cell}^{-1} \text{ day}^{-1}$
VSV	Lysing grate of tumor cells	λ_C	$1 \text{ cell}^{-1} \text{ day}^{-1}$
	Burst size from lysing infected tumor	b_C	1350
	Viral clearance rate	ω	$5.856 \text{ virus}^{-1} \text{ day}^{-1}$
	Uptake/encounter/infection rate of tumor cells	β_C	$1.2 \times 10^{-11} \text{ viruses cell}^{-1} \text{ day}^{-1}$

$$\begin{aligned} \frac{dC_S}{dt} = \Omega_2 C_S(t) \left(1 - \frac{(C_S(t) + C_I(t))}{k} \right) - \psi_2 G(t) C_S(t) \\ - \frac{p_2 C_S(t) Q(t)}{a_2 + C_S(t)} - C_S(t) \beta_C v(t) = 0, \end{aligned} \quad (11)$$

$$\frac{dC_I}{dt} = \beta_C C_S(t) v(t) - \lambda_C C_I(t) = 0, \quad (12)$$

$$\frac{dN}{dt} = \bar{\psi} \dot{G}(t) H(-\dot{G}) N(t) - \frac{p_3 N(t) Q(t)}{a_3 + N(t)} = 0, \quad (13)$$

$$\frac{dQ}{dt} = -\zeta Q(t) = 0, \quad (14)$$

$$\frac{dv}{dt} = b_C \lambda_C C_I - \beta_C C_S(t) v(t) - \omega v(t) = 0. \quad (15)$$

Here, we have taken into account that the chemotherapy infusion Φ is null during the virotherapy. It is obvious that $E_1(0, 0, 0, 0, 0, 0)$ is an equilibrium point. Moreover, the eigenvalues of the corresponding Jacobian matrix are $\lambda_1 = \Omega_1$, $\lambda_2 = \Omega_2$, $\lambda_3 = -\lambda_C$, $\lambda_4 = 0$, $\lambda_5 = -\zeta$ and $\lambda_6 = -\omega$. Note that λ_1 and λ_2 are positive, therefore we have an unstable point. This case is biological unfeasible because we have neither glial cells nor neurons.

A second equilibrium point is $E_2(k, 0, 0, \bar{N}, 0, 0)$, which is the case of a healthy patient without cancer and therapies. Here, we set $\bar{G} = k$ in order to guarantee the equilibrium for the glial cells, and \bar{N} is any real and positive value. The eigenvalues of the Jacobian matrix are $\lambda_1 = -\Omega_1$, $\lambda_2 = \Omega_2 - \psi_2 k$, $\lambda_3 = -\lambda_C$, $\lambda_4 = 0$, $\lambda_5 = -\zeta$ and $\lambda_6 = -\omega$. Note that λ_2 is positive according to the values of Table 1. Therefore, the equilibrium point is unstable. More precisely, if the treatment is ceased

Table 3 Initial, intermediate and final values for glial cells $G(t)$, neurons $N(t)$, tumor cells $C(t)$ and concentration of chemotherapeutic agent $Q(t)$ for the first simulation

	Day 0	Day 21	Day 28
G	5.940×10^{12} cells	5.929×10^{12} cells	5.932×10^{12} cells
N	5.940×10^{12} cells	5.916×10^{12} cells	5.916×10^{12} cells
C with adenovirus	6×10^{10} cells	4.712×10^{10} cells	1.544×10^9 cells
C with HSV	6×10^{10} cells	4.712×10^{10} cells	8.145×10^6 cells
C with VSV	6×10^{10} cells	4.712×10^{10} cells	6.023×10^7 cells
Q	0 mg/m ²	51.72 mg/m ²	12.75 mg/m ²

with some healthy glioma cells $C_S \neq 0$ then the glioma would return. A similar result is established in [17] for the chemotherapy treatment.

4 Simulations and results

In this section, we provide some simulations using the proposed model. Firstly, we provide simulations considering only the chemotherapy treatment from day 0 to day 21, that is, we use Eqs. (1)–(4). From from day 21 to day 28, we will incorporate the virotherapy. The initial, intermediate and final values of the variables are shown in Table 3. Figure 1 shows the evolution of the variables. In particular, we note that the tumor cells results for three different types of virotherapies (there was not significant difference for glial cells or neurons with the three types of virotherapy): adenovirus (ONYX-15) [20,22], HSV [7,22] and VSV [22,30,31].

As a second experiment, in order to search for effects of more chemotherapy sessions, we supplied the virotherapy after the second chemotherapy session, more specifically from day 49 to day 56. The initial, intermediate and final values of the variables are shown in Table 4. Figure 2 shows the evolution of the variables. Similarly to the first experiment, we show the tumor cells results for the three different types of virotherapies. In order to see with more detail the differences among the virotherapies, we show the tumor cells results in logarithmic scale for the two experiments in Figs. 1e and 2e. It is important to remark that at the end of both simulations all the tumor cells are infected by the virus, i. e. $C_S(28) = 0$ for the first simulation and $C_S(56) = 0$ for the second one.

After of an analysis of the simulations we can establish that

- The chemotherapy attacks the tumor very slowly and it would be necessary to supply many sessions to see good results.
- The virotherapy acts faster on the tumor than the chemotherapy.
- There is no significant relevance if we incorporate the virotherapy after the first or the second chemotherapy session.
- Although the result is good for different types of viruses, there is a noticeable difference each other.

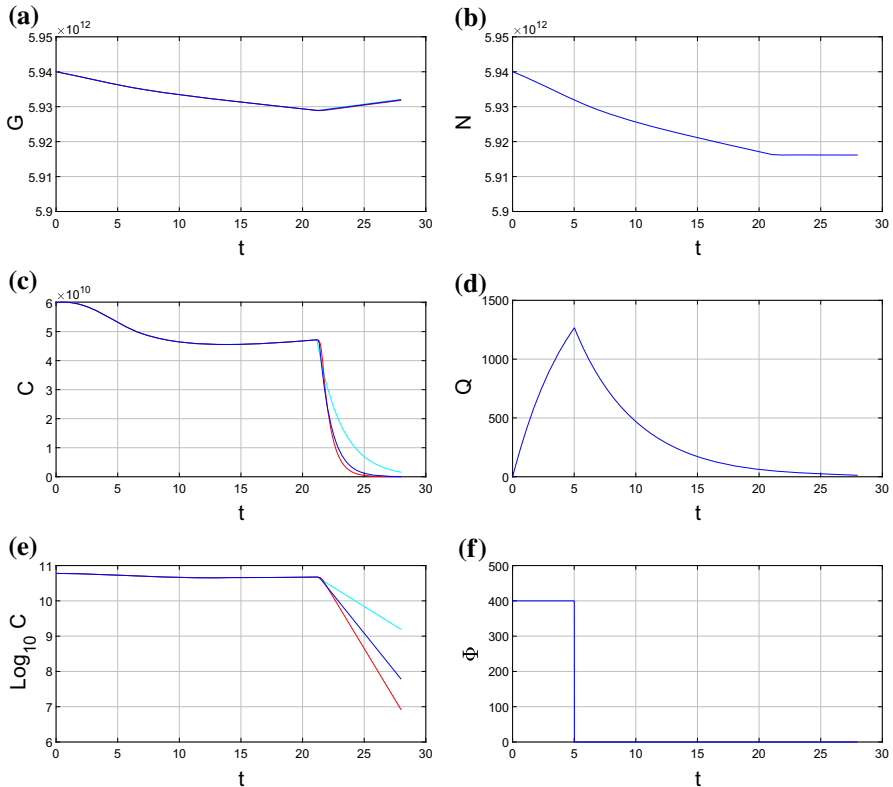


Fig. 1 Results of the first simulation with the temporary variable t in days: **a** number of glial cells G , **b** number of neurons, **c** number of tumor cells with adenovirus (cyan), HSV (red) and VSV (blue) virotherapy, **d** concentration of chemotherapeutic agent in mg/m^2 , **e** the same graphic of **c** but in logarithmic scale and **f** chemotherapy infusion in $\text{mg}/(\text{m}^2 \text{ day})^{-1}$ (Color figure online)

- The simulations present better results for the HSV virus, which is precisely used in glioma treatments [7].
- After the virotherapy, in principle, it would not be necessary to apply more therapies.
- The glial cells and neurons practically are not affected for the chemotherapy, in fact, one can notice a slight recovery of the number of glial cells as a consequence of reduction of glioma cells during the virotherapy.
- The glioma is two or more orders of magnitude smaller at the end of the simulations, in addition, at the same time all the tumor cells are infected by the virus and, as a consequence of this, they do not have capacity of reproduction.

5 Conclusion

In this paper, we propose a mathematical model of a combination of chemotherapy and oncolytic virotherapy as an alternative treatment against cancer, more specifically

Table 4 Initial, intermediate and final values for glial cells $G(t)$, neurons $N(t)$, tumor cells $C(t)$ and concentration of chemotherapeutic agent $Q(t)$ for the second simulation

	Day 0	Day 21	Day 28	Day 49	Day 56
G	5.940×10^{12} cells	5.929×10^{12} cells	5.926×10^{12} cells	5.919×10^{12} cells	5.923×10^{12} cells
N	5.940×10^{12} cells	5.916×10^{12} cells	5.910×10^{12} cells	5.896×10^{12} cells	5.896×10^{12} cells
C with adenovirus	6×10^{10} cells	4.712×10^{10} cells	5.011×10^{10} cells	3.923×10^{10} cells	1.296×10^9 cells
C with HSV	6×10^{10} cells	4.712×10^{10} cells	5.011×10^{10} cells	3.923×10^{10} cells	7.143×10^6 cells
C with VSV	6×10^{10} cells	4.712×10^{10} cells	5.011×10^{10} cells	3.923×10^{10} cells	5.181×10^7 cells
Q	0 mg/m ²	51.72 mg/m ²	12.75 mg/m ²	52.02 mg/m ²	12.83 mg/m ²

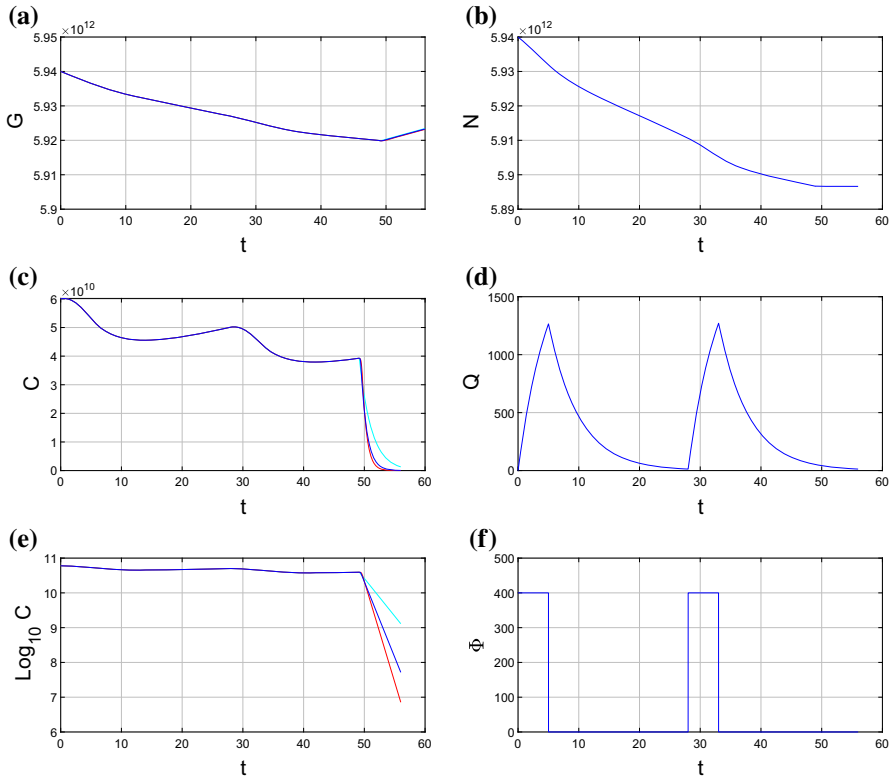


Fig. 2 Results of the second simulation with the temporary variable t in days: **a** number of glial cells G , **b** number of neurons, **c** number of tumor cells with adenovirus (cyan), HSV (red) and VSV (blue) virotherapy, **d** concentration of chemotherapeutic agent in mg/m^2 , **e** the same graphic of **c** but in logarithmic scale and **f** chemotherapy infusion in $\text{mg}/(\text{m}^2 \text{ day})^{-1}$ (Color figure online)

a brain tumor called glioma. The system is based on interactions among glial cells, glioma cells and neurons, including the effects of the corresponding concentration of chemotherapeutic agent. The virotherapy is incorporated by means of the supply of a *specialist* virus that attacks only the tumor cells, in this work we use three different types of viruses. During the virotherapy the tumor cells are divided in healthy and infected, because it is assumed that the infected cells cannot reproduce. The results show that the proposed treatment could reduce the number of chemotherapy sessions and it is recommendable to choose the better kind of virotherapy depending of the type of cancer. Finally, we can conclude that this model strengths the proposals [8–10,32] that claim good results against cancer using a combination of chemotherapy and virotherapy treatments.

Acknowledgements This manuscript is an extended version of a paper presented in July 2019 at the XIX International Conference “Computational and Mathematical Methods in Science and Engineering”, in Rota, Spain. One of us (EUC) wishes to thank CONACYT for the financial support granted through scholarship 390634 and to the Universidad de Guadalajara for PROINPEP support.

References

1. N. Sanai, A. Alvarez-Buylla, M.S. Berger, Neural stem cells and the origin of gliomas. *New Engl. J. Med.* **353**, 811–822 (2005)
2. S.S. Stylli et al., Photodynamic therapy of high grade glioma-long term survival. *J. Clin. Neurosci.* **12**, 389–398 (2005)
3. S. Lonardi, A. Tosoni, A.A. Brandes, Adjuvant chemotherapy in the treatment of high grade gliomas. *Cancer Treat. Rev.* **31**, 79–89 (2005)
4. M. Sturrock, W. Hao, J. Schwartzbaum, G.A. Rempala, A mathematical model of pre-diagnostic glioma growth. *J. Theor. Biol.* **380**, 299–308 (2015)
5. E.S. Newlands et al., Temozolomide: a review of its discovery, chemical properties, pre-clinical development and clinical trials. *Cancer Treat. Rev.* **23**, 35–61 (1997)
6. H.S. Friedman, T. Kerby, H. Calvert, Temozolomide and treatment of malignant glioma. *Clin. Cancer Res.* **6**, 2585–2597 (2000)
7. A. Friedman et al., Glioma virotherapy: effects of innate immune suppression and increased viral replication capacity. *Cancer Res.* **66**, 2314–2319 (2006)
8. A. Nguyen, L. Ho, Y. Wan, Chemotherapy and oncolytic virotherapy: advanced tactics in the war against cancer. *Front. Oncol.* **4**, 145 (2014)
9. G.R. Simpson, K. Relph, K. Harrington, A. Melcher, H. Pandha, Cancer immunotherapy via combining oncolytic virotherapy with chemotherapy: recent advances. *Oncolytic Virother.* **5**, 1–13 (2016)
10. G. Jiang, Y. Xin, J.-N. Zheng, Y.-Q. Liu, Combining conditionally replicating adenovirus-mediated gene therapy with chemotherapy: a novel antitumor approach. *Int. J. Cancer* **129**, 263–274 (2011)
11. T.E. Wheldon, *Mathematical Models in Cancer Research* (Taylor and Francis, London, 1988)
12. L. Preziosi, *Cancer Modelling and Simulation* (Chapman and Hall/CRC, Boca Raton, 2003)
13. W.-Y. Tan, L. Hanin, *Handbook of Cancer Models with Applications* (World Scientific, Singapore, 2008)
14. H. Hatzikirou et al., Mathematical modelling of glioblastoma tumour development: a review. *Math. Models Methods Appl. Sci.* **15**, 1779–1794 (2005)
15. H.L.P. Harpold, E.C. Alvord, K.R. Swanson, The evolution of mathematical modeling of glioma proliferation and invasion. *J. Neuropathol. Exp. Neurol.* **66**, 1–9 (2007)
16. L.E. Ayala-Hernández et al., A mathematical model for the pre-diagnostic of glioma growth based on blood glucose levels. *J. Math. Chem.* **56**, 687–699 (2018)
17. K.C. Iarosz et al., Mathematical model of brain tumour with glia-neuron interactions and chemotherapy treatment. *J. Theor. Biol.* **368**, 113–121 (2015)
18. W. Schuette, Treatment of brain metastases from lung cancer: chemotherapy. *Lung Cancer* **45**, 253–257 (2004)
19. B. Ribba et al., A tumor growth inhibition model for low-grade glioma treated with chemotherapy or radiotherapy. *Clin. Cancer Res.* **18**, 5071–5080 (2012)
20. J.T. Wu, H.M. Byrne, D.H. Kirn, L.M. Wein, Modeling and analysis of a virus that replicates selectively in tumor cells. *Bull. Math. Biol.* **63**, 731–768 (2001)
21. M.A. Nowak, R.M. May, *Virus Dynamics: Mathematical Principles of Immunology and Virology* (Oxford University Press, Oxford, 2000)
22. K.W. Okamoto, P. Amarasekare, I.T.D. Petty, Modeling oncolytic virotherapy: is complete tumor-tropism too much of a good thing? *J. Theor. Biol.* **358**, 166–178 (2014)
23. M. Rajalakshmi, M. Ghosh, Modeling treatment of cancer using virotherapy with generalized logistic growth of tumor cells. *Stoch. Anal. Appl.* **36**, 1068–1086 (2018)
24. S.T.R. Pinho, F.S. Barcelar, R.F.S. Andrade, H.I. Freedman, A mathematical model for the effect of anti-angiogenic therapy in the treatment of cancer tumours by chemotherapy. *Nonlinear Anal.: Real World Appl.* **14**, 815–828 (2013)
25. J.S. Spratt, T.L. Spratt, Rates of growth of pulmonary metastases and host survival. *Ann. Surg.* **159**, 161–171 (1964)
26. F.S. Borges et al., Model for tumour growth with treatment by continuous and pulsed chemotherapy. *BioSystems* **116**, 43–48 (2014)
27. R. Said et al., Cyclophosphamide pharmacokinetics in mice: a comparison between retro orbital sampling versus serial tail vein bleeding. *Open Pharmacol. J.* **1**, 30–35 (2007)
28. C.S. Holling, The functional response of predator to prey density and its role in mimicry and population regulation. *Mem. Entomol. Soc. Can.* **45**, 1–60 (1965)

29. Y. Pei, L. Chen, Q. Zhang, C. Li, Extinction and permanence of one-prey multi-predators of Holling type II function response system with impulsive biological control. *J. Theor. Biol.* **235**, 495–503 (2005)
30. Y. Zhu, J. Yin, Burst size distributions from measurements of single cells infected with vesicular stomatitis virus, in: *AIChE Annual Meeting*. American Institute of Chemical Engineers, Cincinnati, Ohio (2005) 432f
31. D.M. Rommelfanger et al., Dynamics of melanoma tumor therapy with vesicular stomatitis virus: explaining the variability in outcomes using mathematical modeling. *Gene Ther.* **19**, 543–549 (2012)
32. L. Fernandez, L. Orduna, M Perez, J. M. Orduna. A new approach for the visualization of DNA methylation results. *Comput. Math. Methods* (2019). <https://doi.org/10.1002/cmm4.1043>

Publisher's Note Springer Nature remains neutral with regard to jurisdictional claims in published maps and institutional affiliations.